Journal of the Meteorological Society of Japan, Vol. 77, No. 1, pp. 1–16, 1999

Roles of the Western North Pacific Wind Variation in Thermocline Adjustment and ENSO Phase Transition

By Bin Wang, Renguang Wu and Roger Lukas

School of Ocean and Earth Science and Technology, University of Hawaii at Manoa, Honolulu, HI 96822

(Manuscript received 1 June 1998, in revised form 9 September 1998)

Abstract

Analysis of 17 years (1980–1996) of tropical Pacific thermocline variations indicates that short period (about 18 months) cycles in the early 1990s exhibit a relatively small meridional scale. The long period (4–5 year) cycles in the 1980s, associated with major basic-wide warming/cooling events, have much wider meridional scales. The dominant mode of interannual variation of thermocline depth can be approximately described by a basin-scale east-west seesaw oscillation, with an eastward propagation of thermocline depth anomalies occurring in the equatorial waveguide during the transition phases.

The long-period ENSO cycles associated with the major basic-wide warming/cooling events involve a substantial change of heat storage in the western North Pacific (WNP) (5–15°N, 130–170°E). The tendency of thermocline displacement and local wind stress curl in the WNP exhibit a coherent, broad spectral peak on a 8–20 month time scale. The deepening (rising) of the thermocline occurs in phase with the local anticyclonic (cyclonic) wind stress forcing, suggesting the essential roles of the *in situ* wind forcing in thermocline adjustment.

The surface wind variation in the western Pacific is found to play a critical role in the phase transition of ENSO cycles. During the mature phases of major warm episodes, there is a rapid establishment of an anomalous anticyclonic wind stress curl over the WNP. The anticyclonic wind stress deepens the WNP thermocline and starts a recharge of heat content in the warm pool. Meanwhile, the easterly anomalies to the south of the anticyclonic center elevate the thermocline in the equatorial western Pacific, and trigger an eastward migration of the rising thermocline along the equator, leading to cooling in the east. The transition from cooling to warming during the mature phases of cold episodes involves a similar process, but with opposite anomalies.

1. Introduction

Thermocline variations play a critical role in El Niño-Southern Oscillation (ENSO) evolution. They not only "memorize" the effects of Sea Surface Temperature (SST) on winds, but also convey the feedback of the winds to SST in a later time. Due to the paucity of the subsurface observations, however, studies of ENSO have been mostly confined to air-sea interface variables. Among the key parameters describing ENSO, the basin-wide thermocline adjustment during ENSO cycles is not well known.

Irrespective of the observational limitations, tremendous efforts have been made to describe and understand the subsurface variability associated with ENSO using either the output generated from the ocean general circulation model (Chao and Philander, 1993) or the observed 20°C isotherm depth, sea-level height, and upper ocean heat storage (Firing *et al.*, 1983; Lukas *et al.*, 1984; White *et al.*, 1985, 1989; Kessler, 1990; McPhaden *et al.*, 1990; Tourre and White, 1995; Kessler and McPhaden, 1995; Chelton and Schlax, 1996; Boulanger and Fu, 1996; Zhang and Levitus, 1997). These analyses have demonstrated important roles of oceanic waves in thermocline adjustment and the roles of thermocline variation in affecting ENSO cycles. Some of these analyses, however, had limitations arising from: insufficient basin-wide data coverage; the coarse temporal resolution (yearly mean); the spatial unevenly distributed observations; and the insufficient length of data records. These limitations sometimes posed serious problems in a description of detailed evolution of basin-wide thermocline adjustment during ENSO cycles with variable periodicity.

Corresponding author: Prof. Bin Wang, School of Ocean and Earth Science and Technology, University of Hawaii at Manoa, 2525 Correa Road, Honolulu, HI 96822. E-mail: bwang@soest.hawaii.edu

The latest version (RA 6) of the subsurface data produced by the NCEP (National Center for Environmental Prediction) Ocean Data Assimilation System (ODAS) provides an unprecedented opportunity for examination of the thermocline variability for the period 1980 to 1996. Although the length of the assimilated data record remains limited, the data contains two relatively long ENSO cycles in the 1980s and three short cycles in the first part of the 1990s. The latter appear to evolve in a background which has experienced decadal variation (Wallace *et al.*, 1997). As such, the later portion of the period distinguishes from the first decade of the data by a broadening of the spectrum. It is interesting to find out whether the thermocline variation differs between the long and short ENSO cycles. The purpose of addressing this question is to identify possible decadal variation in ENSO evolution and the factors which determine the oscillation period in subsurface "memory" of the ocean.

A major thrust driving this study is to investigate the roles of the thermocline adjustment in the transition from warming to cooling trends, or vice versa of the ENSO cycles. The cause of the turnabout, or the cause of the irregular cyclic nature, has been a controversial issue in the past three decades since Bjerknes (1969). Thermocline variations associated with equatorial Kelvin waves were suggested to play important roles in the onset of the El Niño (*e.g.*, Wyrtki, 1975; Harrison and Schop, 1984; Lukas *et al.*, 1984), while the equatorially trapped and off-equatorial Rossby waves have been suggested by numerous studies to play critical roles in the turnabout of the ENSO cycles, but with notable debates (*e.g.*, White *et al.*, 1985, 1989; Kessler, 1991; Li and Clarke, 1994; Mantua and Battisti, 1994; Kessler and McPhaden, 1995). These debates concern the validity of the delayed oscillator theory put forward by Schopf and Suarez (1988), Suarez and Schopf (1988), and Battisti and Hirst (1989) in explaining the mechanism of the quasi-regular oscillation of ENSO.

The existing coupled models have produced a variety of behaviors of interannual oscillations with period ranging from two years (Ineson and Davey, 1997) to five years (Philander *et al.*, 1992) or longer. All these numerical model-produced oscillations were claimed to bear some degree of similarity to the observed ENSO. It is necessary to ask what are the fundamental characteristics of ENSO evolution in terms of thermocline displacement, or heat storage redistribution, which can be used to validate numerical model simulation. The analysis of the ODAS subsurface temperature variation may provide useful guidance.

Section 2 discusses the definition of thermocline depth, followed by a description of fundamental characteristics of the basin-scale thermocline adjustment during ENSO cycles (Section 3). The composite evolutions of ENSO cycles in the 1980s and 1990s are then compared in Section 4. Section 5 focuses on key processes determining the thermocline variation in the western North Pacific — one of the key regions in the interannual thermocline variation. Section 6 discusses the processes which are possibly responsible for ENSO phase transitions. The last section presents a summary and alternative hypothesis regarding the turnabout mechanism, and discusses remaining issues and implications of the results.

2. Data and definition of the thermocline depth

The ocean temperature data used in the present study were derived from the latest version (RA6) of the data set assimilated at the NCEP (Ji *et al.*, 1995), from January 1980 to December 1996. The ocean data assimilation system uses nearly all the available temperature observations throughout the basin and the GFDL (Geophysical Fluid Dynamics Laboratory) ocean general circulation model physics, to provide a three-dimensional description of dynamically and thermodynamically consistent ocean fields. The observations used include SST measured from ships, buoys, and satellites, and subsurface temperature measured from moored buoys and expendable bathythermographs.

Monthly mean time series are first computed for each of 1° latitude by 3° longitude grid to eliminate small scale noise and to increase computational efficiency. To describe vertical displacement of the thermocline, we computed two variables. One is the upper ocean heat storage (HS), which is defined by the vertical integration of temperature from surface to 400 m depths. The other is the "thermocline depth" defined by the depth of a specific temperature representing the central location of a local thermocline layer, Tc. The temperature Tc is the average of the local long-term mean SST and 12°C (the mean temperature at 350 m over the tropical region between 20°N and 20°S) (Wang *et al.*, 1998). Between 20°N and 20°S, Tc varies from about 20°C in the warm pools to 16°C in the cold tongue near the Peru coasts. The depth of Tc is a reasonable representation of the depth of the interface in an equivalent two-layer system and of the upper ocean dynamical response to surface wind forcing. The monthly mean thermocline depth anomaly (TDA) defined by the above definition, and the monthly mean heat storage anomaly (HSA), are highly correlated with a correlation coefficient exceeding 0.8 all over the tropical Pacific between 20°N and 20°S except the southeastern Pacific (Fig. 1a). In the areas where the thermocline displacement has the largest variability, *i.e.*, the equatorial eastern Pacific and off-equatorial western Pacific warm pool (Fig. 1b), the correlation coefficient is higher than 0.95. Paral-

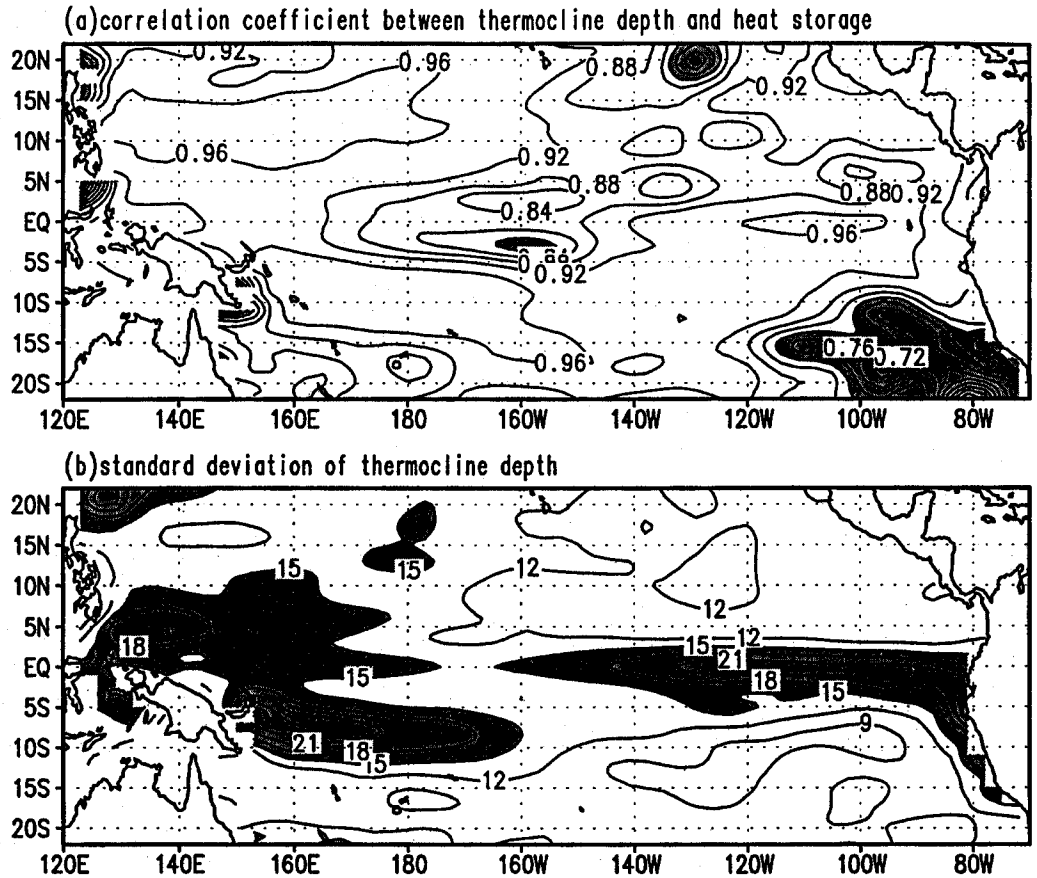

Fig. 1. (a) Correlation map showing the correlation coefficient between the thermocline depth and heat storage anomalies; (b) Standard deviation of the thermocline depth anomalies (m). The data are monthly mean anomalies derived from NCEP reanalysis (Ji *et al.*, 1995).

lel analyses of TDA and HSA have been carried out and the differences are qualitatively insignificant.

Monthly mean anomalies (MMAs) are obtained by subtracting the climatological annual cycle from the original monthly means. The MMAs are used to depict the Rossby wave propagation (Fig. 6). We also apply a 5-month running mean to the MMAs in order to isolate interannual variations. This filter retains more than 50% variances for the oscillation with periods longer than 10 months, while sub-annual variations are largely removed. To focus on the variation associated with ENSO, the 5-month running means are further decomposed into an ENSO component and a decadal component. The decadal component is defined by the sum of the Fourier harmonics with periods longer than seven years, while the ENSO component is the difference between the 5-month running mean anomalies and the decadal component.

3. Characteristics of the tropical Pacific basin-wide thermocline adjustment

The most important variables describing key processes of the ocean-atmosphere interaction are sea surface temperature (SST), surface zonal and meridional winds, and thermocline depth. An analysis of their joint variations is performed using the ENSO components of the monthly mean anomalies. Figure 2 displays the spatial patterns and corresponding principal components of the first two multi-variate empirical orthogonal function (MV-EOF) modes. The first two modes are well separated from the other modes according to the North *et al.* (1982) criterion and they represent, respectively, 31.9% and 12.5% of the total variance of the monthly mean anomalies of all four fields. The large difference between the percent variances explained by the first two modes implies that the coupled interannual variation of SST, wind stress and thermocline, exhibits a prominent *standing* component. The fractional variances (Wang, 1992) explained by MVEOF1 for SST, surface zonal and meridional wind, and thermocline depths are 56.1%, 26.7%, 18.8%, and 26.0%, respectively. This suggests that the largest contribution to the standing component is SST variation.

The first EOF mode (Fig. 2a) depicts the peak warming/cooling phase of ENSO as indicated by its associated temporal coefficient, shown in Fig.

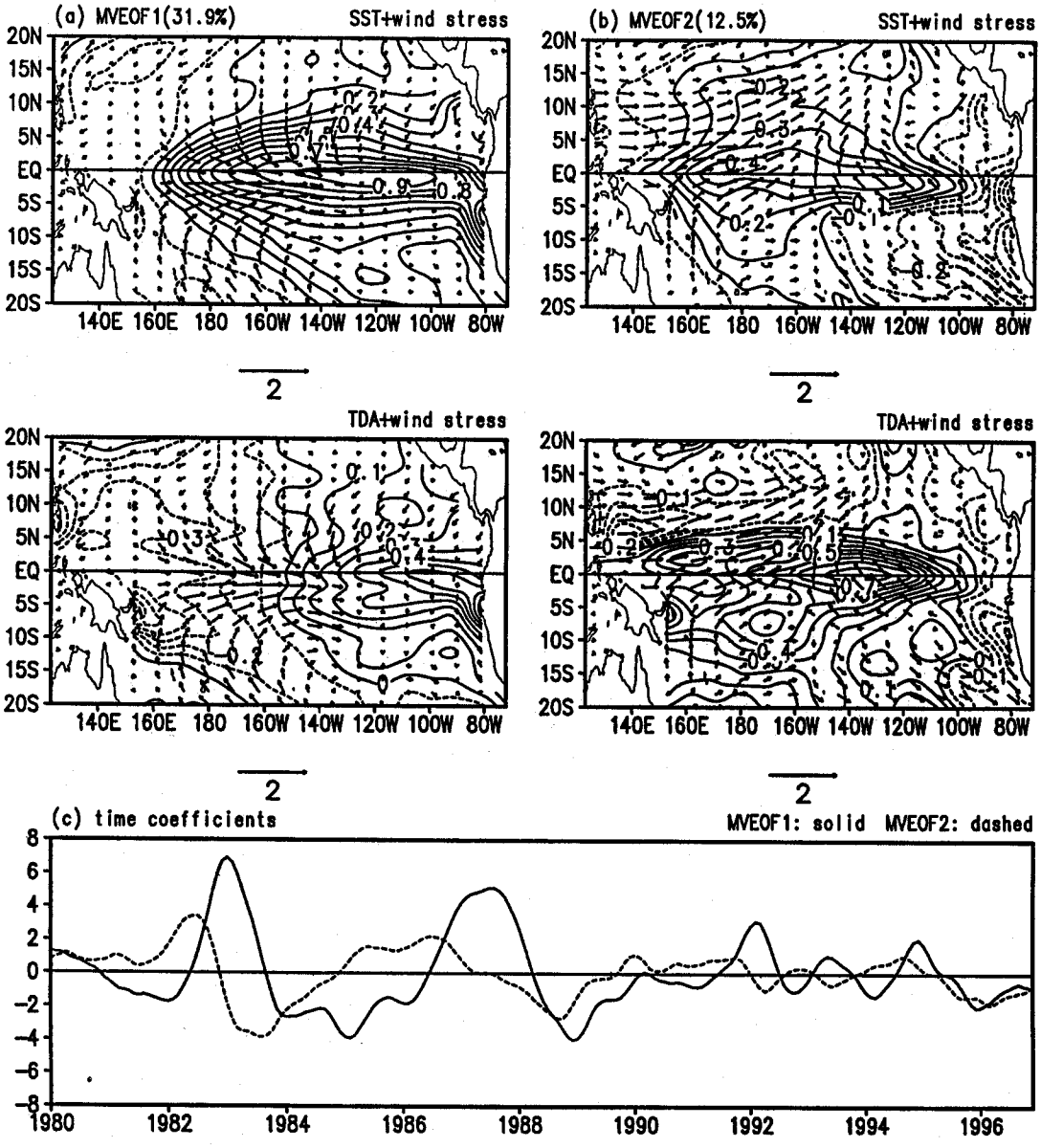

Fig. 2. (a) The spatial structure of the first Multi-Variate EOF mode: the anomalous SST (°C) and surface wind stress (the upper panel) and the anomalous thermocline depth (m) and surface wind stress (the lower panel); (b) the same as in (a) except for the second EOF mode; (c) the corresponding time coefficients for the first (solid) and second (dashed) EOF mode. The data used are the ENSO component of monthly mean anomalous SST, surface wind stress, and thermocline depth derived from the NCEP reanalysis. The definition of ENSO component is referred to the text.

2c. The *peak warming* is characterized by (a) not only the pronounced positive SST anomalies in the equatorial eastern-central basin, but also the moderate negative anomalies centered in the off-equatorial western North and South Pacific, and (b) positive TDAs in the equatorial eastern Pacific and negative TDAs in the off-equatorial western Pacific. The triple action centers in the thermocline anomaly are dynamically consistent with the equatorial central Pacific westerly anomalies and associated cyclonic wind stress curl on each side of the equator. These stimulate westward propagating upwelling Rossby waves, and eastward propagating downwelling Kelvin waves. The equatorial westerly anomalies are consistent with eastward anomalous equatorial SST gradients.

The second EOF mode leads the first by a fraction (about a quarter) of the cycle (Fig. 2c). It approximately depicts the *transient phases* from cold to warm states for the significant warm episodes (1982/83, 1986/87, 1991/92 and 1994). The *transient phase* features a meridional contrast in TDAs between the equatorial belt (5°N–5°S) and the off-equatorial latitude band between 5°N and 15°N.

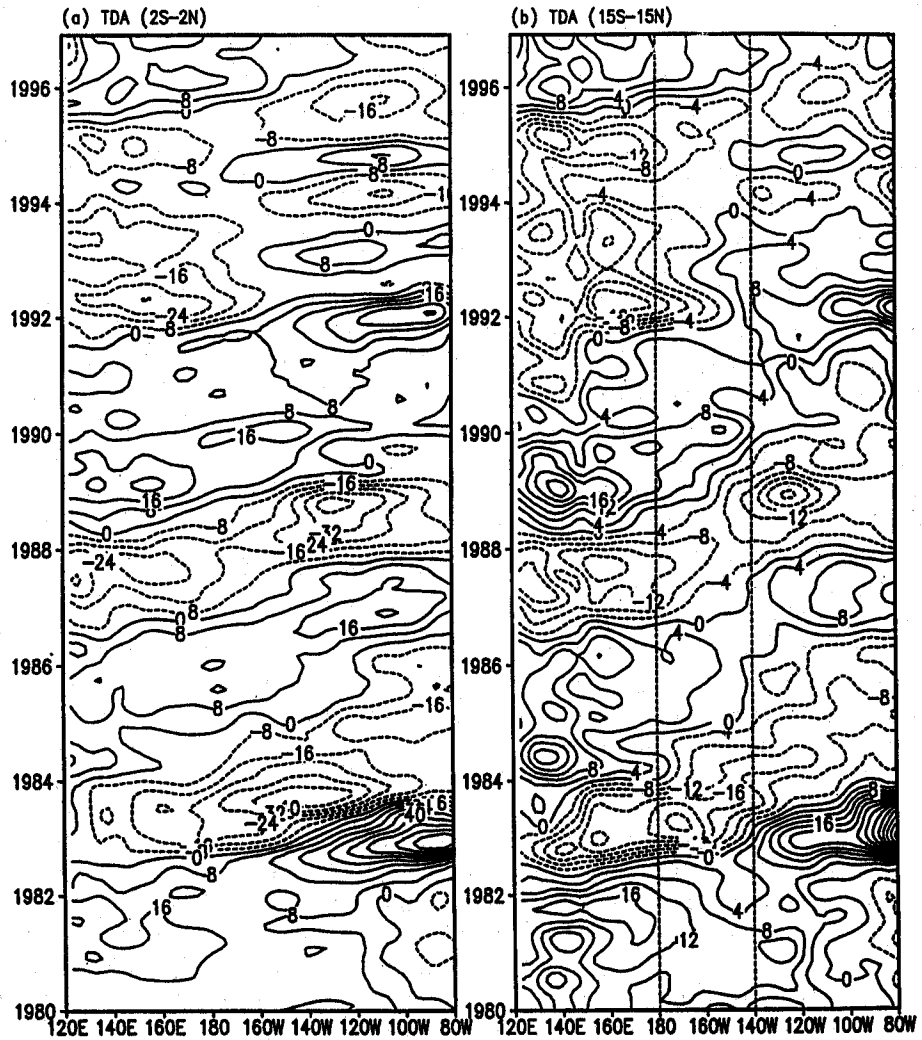

Fig. 3. Hovemöller diagrams of the 5-month running mean thermocline depth anomalies (m) along 2°S–2°N (a) and 15°S–15°N (b).

This meridional thermocline slope is associated with an unusually strong North Equatorial Counter Current (Wyrtki, 1974).

The deepening of the zonal mean thermocline along the equator leads the mature phase of warming by about a quarter of a cycle. This feature was first noticed by Zebiak and Cane (1987) in their coupled model. This characteristic of the ENSO cycle may be used as a precursor for eastern Pacific warming. Monitoring the equatorial zonal mean thermocline depth variation appears to be critical for ENSO prediction (Wyrtki, 1984).

During the transient phases of the ENSO cycle, the thermocline anomalies propagate eastward in the equatorial waveguide (Fig. 3a). The propagation speed is much slower than that of oceanic Kelvin waves. It is a manifestation of the basin-wide thermocline adjustment associated with the coupled ENSO mode. The eastward propagation tends to be narrowly trapped to the equator within 4°N and 4°S. When TDAs are averaged over a broad band between 15°N and 15°S (about one atmospheric Rossby radius of deformation on each side of the equator), the eastward propagation occurs only in the central Pacific from the dateline to 140°W, and during the long cycles in the 1980s. In the western (120°E–180°E) and the eastern (140°W–80°W) basins the thermocline varies nearly in phase (stationary), but the thermocline variations between the east and western basins are almost precisely out of phase (Fig. 3b). Therefore, to the lowest order approximation, the basin-wide thermocline adjustment between 15°S and 15°N can be viewed as a standing oscillation (Wang and Fang, 1996).

4. Differences in ENSO thermocline adjustment between 1980s and early 1990s

The decade of the 1980s was dominated by two large-amplitude ENSO cycles with 4–5 year periodicity, while the early part of the 1990s features

three small-amplitude cycles with periods of about 18 months (Fig. 2c). If lag correlation maps are used, the derived results will be dominated by the two long cycles. For this reason, we examine thermocline evolution during each individual cycle according to their phases. For convenience, eight phases are defined in terms of the time coefficient of the first MVEOF mode, $C_1(t)$ (Fig. 2c). The maximum and minimum of $C_1(t)$ define, respectively, the peak warm and peak cold phases, while the zeros of $C_1(t)$ mark the transient phases. The other four phases can be linearly interpolated between the corresponding transient and extreme phases and, for convenience, are simply referred to as the onset and decay of warm (cold) as appropriate. The time intervals between two defined adjacent phases are not equal, because the evolution is not sinusoidal and the oscillation period may change from cycle to cycle. Note also that the MVEOF modes in Fig. 2 are derived from the ENSO component (time scale longer than one year, but less than seven years). The time coefficient $C_1(t)$ is thus not affected by the decadal variation. Consequently, the warming and cooling are nearly symmetric around the mean in the 1990s. If the decadal variation is added to the ENSO component, the short cycles in the early 1990s may be viewed as fluctuations within a prolonged warm phase from 1991–1994, because the weak cooling around October 1992 and February 1994 was offset by the decadal warm phase in the 1990s.

The evolution of each ENSO cycle was examined using eight-phase diagrams. It was found that the two long cycles in the 1980s share many common features. So do the three short cycles. To compare the features associated with the long and short cycles, two composite cycles were constructed from the ENSO component (not the first two MV-EOFs), one for the long cycles (Fig. 4a) and the other for the short cycles (Fig. 4b).

Notable differences exist between the composite long and short cycles. First, for short cycles, not only is the amplitude substantially smaller, but the locations of major anomalies also tend to be more tightly trapped near the equator, *i.e.*, *the short cycle has a significantly smaller meridional scale*, especially in the western Pacific. Another difference lies in the thermocline variation in the off-equatorial regions. For the short cycle, the off-equatorial TDA tends to amplify and anchor in the central North Pacific around 10°N, 140–170°W during non-peak phases (Fig. 4b). The TDA in that region tends to be out-of-phase with that in the equatorial eastern Pacific, suggesting that short cycles involve a significant component of half-basin scale. For long cycles, the TDA tends to develop in the western North Pacific, and involves a substantial change of heat storage in the off-equatorial warm pool regions. Last, for the long cycles, there is a poleward spread of TDA in the far eastern basin during the decay phases of warming or cooling, which was absent during the short cycles.

Regardless of the differences, common features are seen in Figs. 4a and 4b: the eastward propagation of TDA along the equator during the transient phases; and, (ii) the east-west dipole during the mature warm and cold phase. In addition, during the transient and onset phases, the off-equatorial TDAs are primarily formed in the Northern Hemisphere. The last feature may be subject to interdecadal variation. Before 1980, the thermocline variation in the Southern Hemisphere was as large as in the Northern Hemisphere, as shown in Chao and Philander's (1993) analysis of the model simulated thermocline evolution for the period 1969–1978.

5. Thermocline variations in the western North Pacific

The most prominent interannual variations in thermocline displacement are found in the equatorial eastern Pacific and off-equatorial western Pacific warm pool (Fig. 1b). The WNP warm pool is one of the key regions in thermocline evolution. Based on observations taken before 1981, Meyers (1982) noticed a negative correlation between the sea level height at Truk (7.4°N, 151.8°E) and the equatorial eastern Pacific SST. As shown in Fig. 5, this relationship remains valid after 1980. The thermocline rising (deepening) in the WNP (5–15°N, 130–170°E) tends to be in phase with equatorial eastern Pacific warming (cooling). This section discusses the possible cause of the thermocline variability in the WNP warm pool, and the next section discusses the potential roles of this variability in maintaining ENSO cycles.

5.1 What controls the thermocline variation in the WNP?

Previous studies have suggested that the TDAs in the WNP result from the anomalies generated in the central-eastern North Pacific through Rossby wave propagation (*e.g.*, Graham and White, 1988; Kessler, 1990; Zhang and Levitus, 1997). The composite thermocline evolution (Fig. 4) shows some evidence of westward propagation of thermocline anomalies from the central North Pacific (CNP) to the WNP. However, Fig. 4 also shows evidence of *in situ* development of thermocline anomalies in the WNP which must be attributed to local wind stress curl forcing.

To examine westward propagating Rossby waves, we present longitude-time diagrams of TDA along different latitude bands across the North Pacific basin (Fig. 6). The data used are monthly mean TDA anomalies, which are adequate to resolve propagation of Rossby waves. Along 4°N, the Rossby

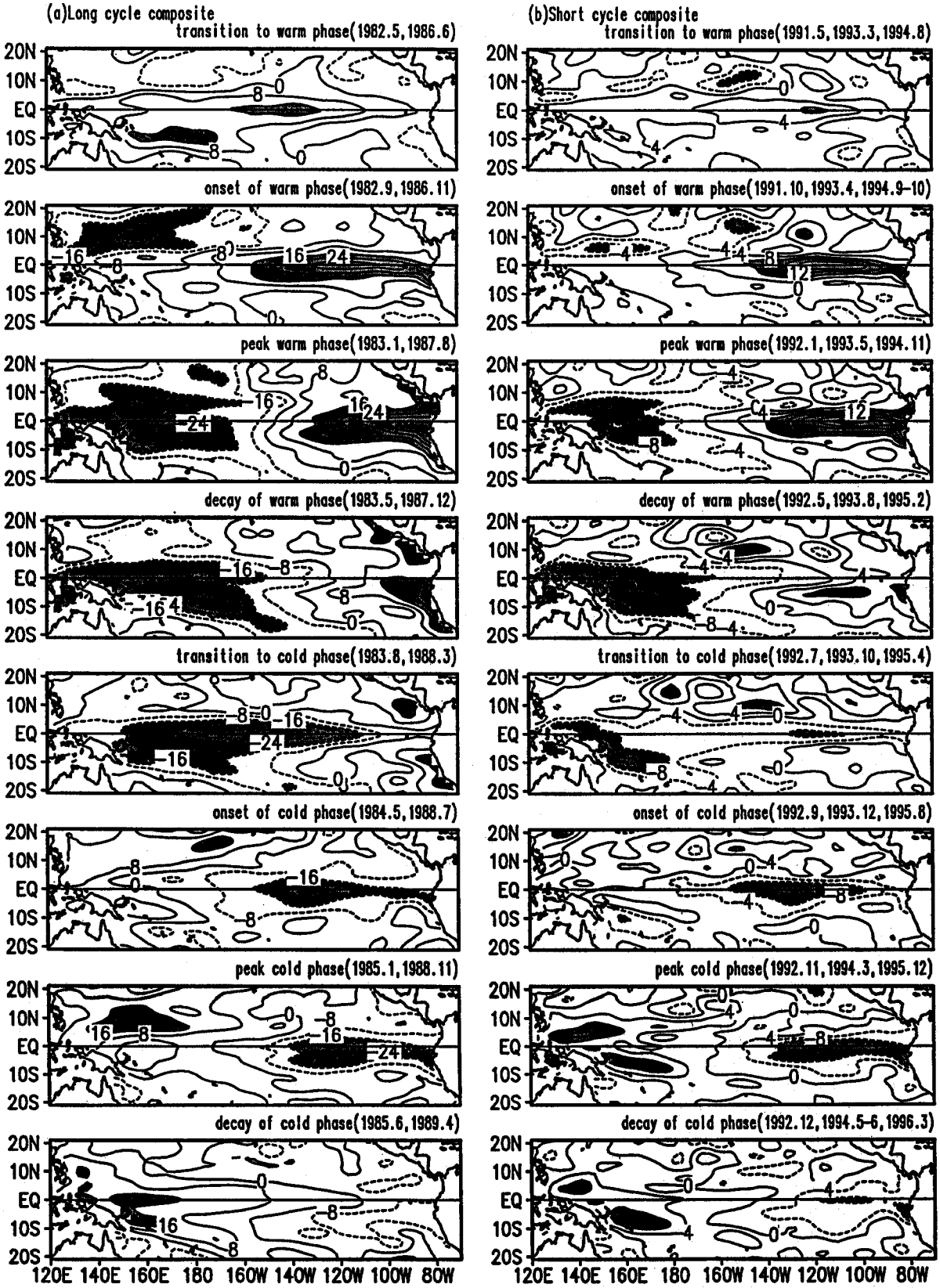

Fig. 4. Composite life cycle of thermocline depth anomalies (m) for (a) the two long cycles from June 1982 to February 1990, and (b) the three short cycles from July 1991 to May 1995. The data used are the same as in Fig. 2. Note the different contour intervals used in (a) and (b).

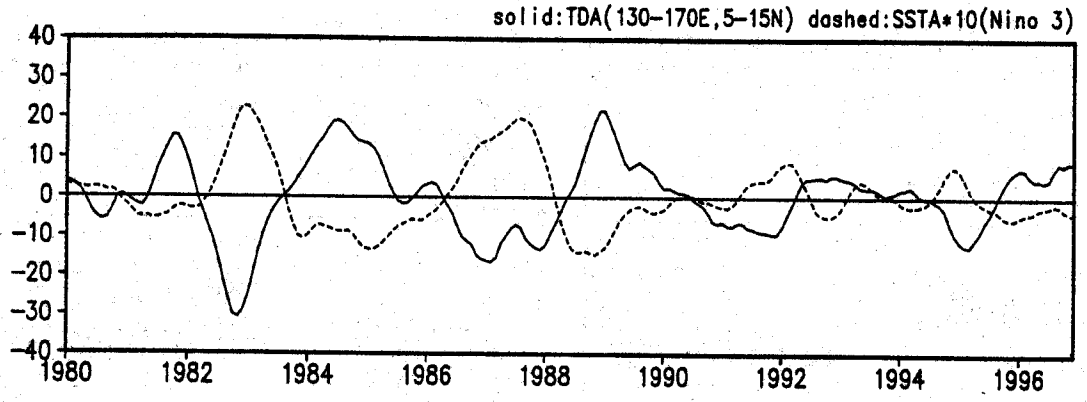

Fig. 5. Thermocline depth anomaly (m) averaged over the area 130°E–170°E, 5°–15°N (solid) and Nino 3 SST anomaly (0.1°C) (dashed). The data used are the same as in Fig. 2.

wave propagation is evident on the annual time scale (*cf.*, Chelton and Schlax, 1996), but not on the interannual time scale (Fig. 6). The westward propagation of TDA is also not seen in the latitude band along 5–6°N (Fig. 6). Sporadic episodes of the westward propagation of TDA can be seen along 7–8°N, but the propagation rarely reaches the western ocean boundary. This raises a question regarding the critical roles of the equatorial Rossby wave reflection at the western boundary in the ENSO turnabouts. Along the latitude bands between 9°N and 15°N, however, westward propagation of TDA associated with major ENSO cycles can be identified (Fig. 6). The propagation speed decreases with latitude as expected from the theory. Figure 6, therefore, indicates that the contribution to WNP TDA of Rossby wave propagation from the central Pacific increases with latitude, primarily beyond 8°N.

While the ocean Rossby wave can play certain roles in the thermocline adjustment in the WNP, there is substantial *in situ* development of TDA associated with local wind stress forcing. The WNP (5–15°N, 130–170°E) surface wind stress curl displays a statistically significant broad spectral peak on a time scale between 8 and 20 months (Fig. 7a). This broad energy peak in the surface winds appears to be consistant with the finding of Yanai and Li (1994). Although the thermocline variation in the WNP is overshadowed by ENSO cycle (Fig. 5), the thermocline depth *tendency* shows a similar broad spectral peak with concentration of variances on time scales about 9 and 15 months (Fig. 7b). This is coherent with the variations in the local surface wind stress curl (Fig. 7c). The coherency in the wind and thermocline depth tendency suggests that the thermocline depth variations are responding to the surface wind variations. The important roles of the local wind stress curl in controlling thermocline displacement should be emphasized.

Figure 7 implies that the local wind stress forcing is potentially a major contributor to changes in thermocline (or heat storage) in the WNP. The importance of the local wind forcing can be further substantiated by the negative correlation between the tendency of thermocline depth, and local wind stress curl (Fig. 8a). The correlation coefficient between the tendency of thermocline depth and local wind stress curl is −0.63 for the period January 1980 to December 1996. Our estimations show a decorrelation time scale of about 4 months and a degree of freedom of 50 (Livezey and Chen, 1983), indicating that the correlation is significant at a confidence level more than 99.9%. Figure 8a indicates that deepening (rising) of thermocline tends to be in-phase with local anticyclonic (cyclonic) wind stress curl in the WNP. This is a result of baroclinic adjustment of the thermocline to wind stress forcing through Ekman pumping. Anticyclonic (cyclonic) wind stress curl induces downward (upward) motion in the Ekman layer which deepens (elevates) the thermocline. In addition to the baroclinic adjustment, anticyclonic wind stress may also favor heat storage by affecting thermodynamic processes and horizontal advection of heat. The low cloudiness associated with the anticyclonic circulation would increase solar radiation at the surface, while the low wind speed associated with the anticyclonic circulation would reduce the heat loss at the surface, both favoring the accumulation of heat in the WNP. The anticyclonic wind stress curl may also change the strength of the subtropical and equatorial gyre circulation. The latter, especially the Mindanao Current and the North Equatorial Countercurrent may affect heat storage in the WNP (Lukas, 1988; Qiu and Lukas, 1996).

The results showed in Figs. 7 and 8a indicate that *local wind stress forcing is likely a major contributor to changes in the heat storage in the western North Pacific.*

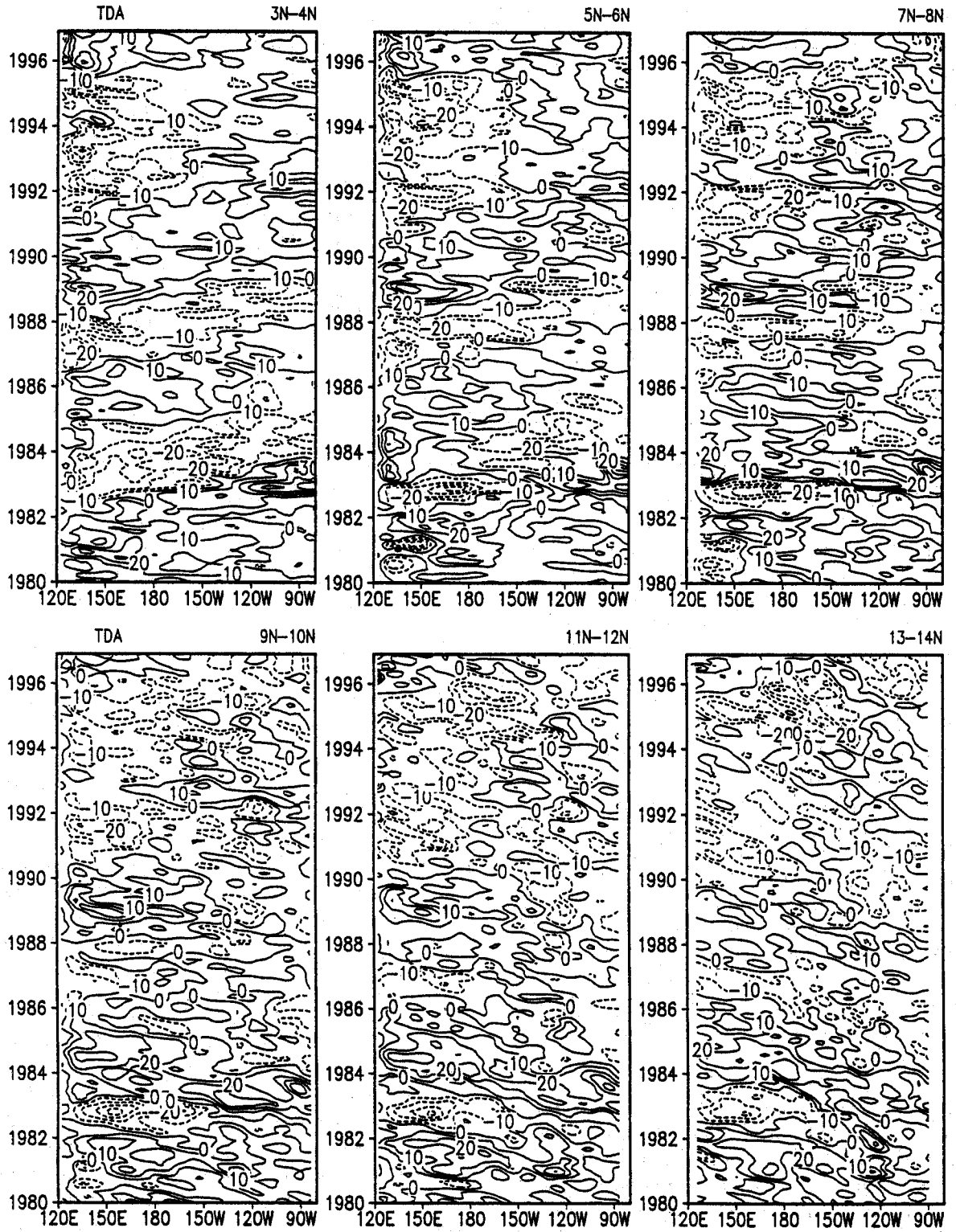

Fig. 6. Hovemöller diagrams of monthly mean thermocline depth anomaly (m) along 3°N–4°N, 5°N–6°N, 7°N–8°N, 9°N–10°N, 11°N–12°N, and 13°N–14°N.

5.2 How is the WNP warm pool "recharged"?

The process of accumulating heat in the WNP consists of two stages: a *relatively rapid restoration* from a minimum to normal heat content, and a continuing but slower *build up* from normal to a maximum. The rapid restoration often occurs following a major peak warming (*e.g.*, January 1983, December 1987, January 1992, and December 1994) (Fig. 5a). This rapid restoration is largely caused by an anticyclonic wind stress curl developed locally over

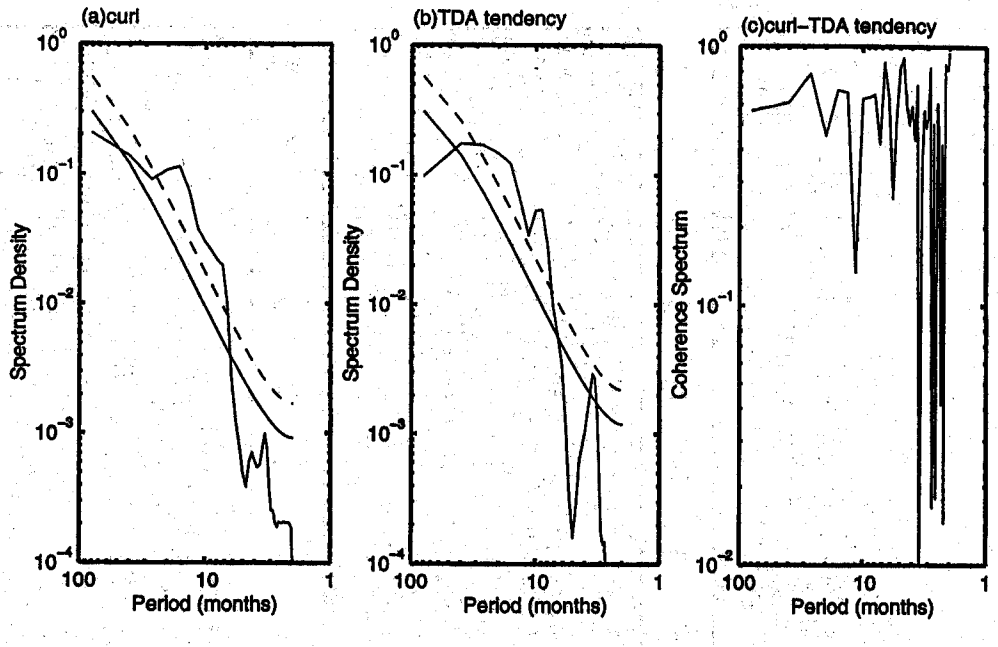

Fig. 7. Spectrum of (a) the surface wind stress curl and (b) the tendency of the thermocline depth anomalies averaged over the western North Pacific (130°E–170°E, 5°N–15°N) and (c) their coherence spectrum. The solid and the dashed curves are the red-noise spectrum and 95% confidence level. The data used are 5-month running means.

the WNP concurrent or following each major peak warming (Fig. 8a solid curve).

The continuing build up of heat storage does not necessarily follow the rapid restoration. An example is found in 1992. After the 1991–92 warm event, there was a short period of restoring heat in the WNP, but no continuing build up (deepening of the thermocline) followed (Fig. 5a). This is, to a large extent, due to influence from a rapid decadal phase change around 1990 in the western and central Pacific (Wallace *et al.*, 1997). In the 1990s, a weak, persistent cyclonic wind stress curl was observed in the WNP (in association with the westerly anomalies persisting in the equatorial western Pacific), which prevented the build up of heat.

The build up of heat in the WNP is also not necessarily preceded by a rapid restoration. An example can be found in 1981 during which the deepening of the thermocline started from a near normal condition. This implies that the 1982/83 warm episode occurred without being preceded by significant cooling. The break of the linkages between the rapid restoration and continuing build up of heat storage in the WNP results in irregularities in the ENSO cycles and difficulties for ENSO prediction.

Note also that the build up of heat in the WNP does not depend on anomalous equatorial easterlies. In fact, the correlation between anomalous equatorial easterlies in the central-eastern Pacific, and the anticyclonic wind stress curl over the WNP is rather low (figure not shown).

6. ENSO transition from peak warm to cold phases

What causes the turn about from a peak warm phase to the subsequent cold phase? This is the question which Bjerknes (1969) raised in his influential paper, and it has remained an unresolved issue. The delayed oscillator theory (Schopf and Suarez, 1988; Suarez and Schopf, 1988; Battisti and Hirst, 1989; Cane *et al.*, 1990) explains the transition from warming to cooling as a result of equatorial thermocline adjustment due to wave propagation. During the warming, the anomalous equatorial westerlies in the equatorial central Pacific create cyclonic wind stress curl in each side of the equator. This in turn generates westward propagating, upwelling Rossby waves. These Rossby waves, upon reflecting from the western boundary, project on to equatorial upwelling Kelvin waves propagating eastward, raising the eastern Pacific thermocline and eventually leading to reversal of the warm state. This explanation implicates equatorial trapped Rossby wave reflection as the trigger of the transition from a warm to a cold phase. While in the simple type of coupled ocean-atmosphere models, the motion in the WNP corresponds primarily to free oceanic waves. This may not be the case in the reanalysis data, as shown in the previous section (Figs. 7 and 8a). From the observed thermocline variation, the westward propagating Rossby waves are not evident equatorward of 7°N (Fig. 6). In theory, effective generation of Kelvin waves due to Rossby wave reflection against

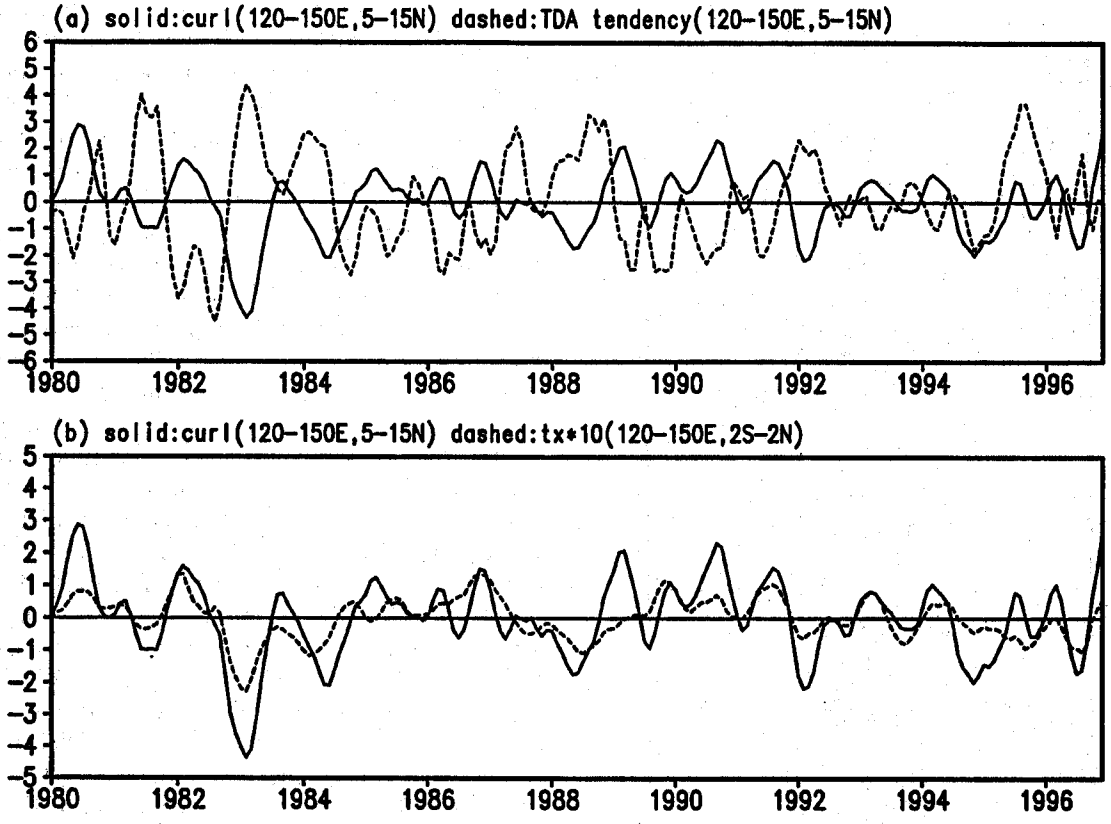

Fig. 8. (a) Monthly mean of surface wind stress curl anomalies (solid, in units of 10^{-9} dyn/cm^3) and the tendency of the TDA (dashed, in units of m/month) averaged in the western North Pacific (120°E–150°E, 5°N–15°N). (b) Monthly mean surface wind stress curl anomalies (solid) averaged over the western North Pacific and the zonal wind stress (0.1 dyn/cm^2) averaged over the equatorial western Pacific (120°E–150°E, 2°S–2°N). The data used are 5-month running means.

a western ocean boundary comes primarily from the Rossby waves within 7° latitudes from the equator (Battisti, 1989). The results shown by Fig. 6 imply that the Rossby wave reflection at the western boundary, as seen from the reanalysis data, may not provide a sufficient negative feedback to turn the coupled system from a warm to a cold phase.

Based on the present analysis of the observed subsurface temperature variations, we found that an alternative mechanism may be at work. The transition from peak warming (cooling) to a cold (warm) phase is triggered by the *anomalous anticyclonic (cyclonic) wind stress curl* developed locally over the WNP. We describe a scenario of transition from a peak warm to a cold phase, for convenience of the discussion.

During the peak phase of a major warm event (for instance, those that occurred around January 1983, late 1987, January 1992, and December 1994 in Fig. 5a), the wind stress curl over the WNP rapidly changes from cyclonic to anticyclonic. A few months later, strong anticyclonic wind stress curl was established over the WNP in spring 1983, spring 1988, spring 1992, and spring 1995 (Fig. 8a solid curve). The anomalous anticyclonic wind stress curl induces Ekman downwelling and thermocline deepening in the WNP, which terminates the discharge of heat content in the WNP warm pool (corresponding to the rapid restoration of heat content described in Section 5). Associated with the anomalous anticyclonic winds are anomalous easterlies to the south of the anticyclone center in the equatorial western Pacific (EWP) (Fig. 8b). The equatorial easterly anomalies (occurred in spring 1983, summer 1988, early 1992, and spring 1995) raise the thermocline in the EWP. An eastward propagation of elevated thermocline along the equator then follows (Fig. 3a) and leads to the decay of the equatorial eastern Pacific warming.

Concurrent with the restoration of heat content in the WNP and the maximum rising in the EWP, there is a meridional redistribution of heat in the eastern Pacific which can be seen from the poleward propagation of the positive TDAs along 90–110°W during the decay of the warming (Fig. 9). This confirms the result of Chao and Philander (1993), who found a similar poleward propagation during the period 1969–1978 from analysis of the simulation us-

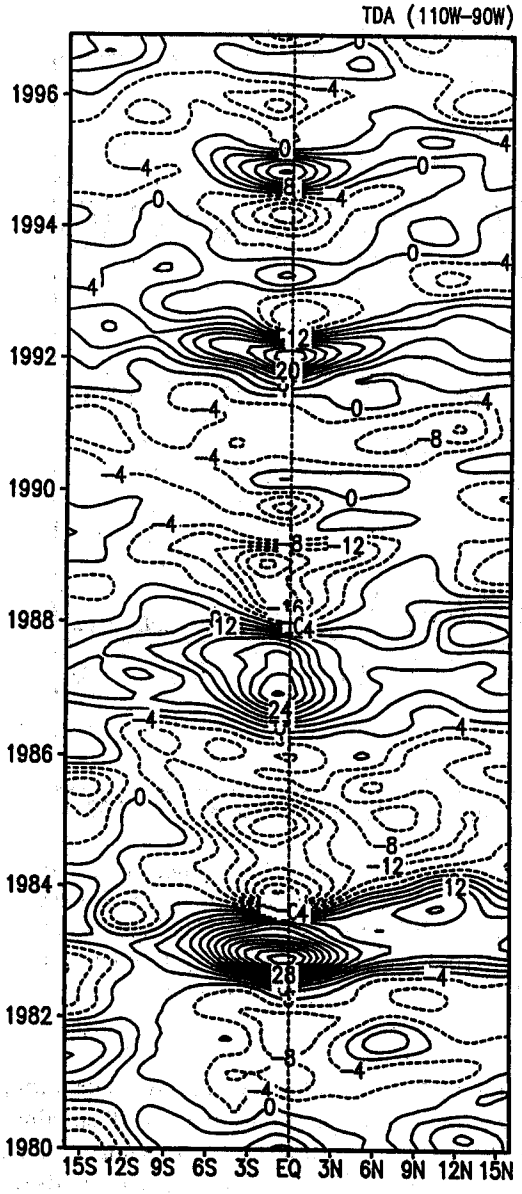

Fig. 9. Time-latitude diagram of the thermocline depth anomalies (m) averaged between 110°W and 90°W. The data used are the same as in Fig. 2.

ing the GFDL (Geophysical Fluid Dynamics Laboratory) ocean general circulation model. This redistribution of heat is primarily due to poleward downwelling coastal Kelvin waves and associated Rossby waves reflected from the eastern boundary, which can efficiently remove heat content from the equatorial eastern Pacific as indicated in Fig. 4.

The rise of thermocline in the east favors decay of warming which in turn increases zonal SST gradients and restores equatorial easterlies. As a result, the westward wind stress over the central equatorial Pacific strengthens. Thus, the elevated thermocline (negative thermocline depth anomalies) in the EWP starts to migrate eastward slowly along the equator (Fig. 4) and eventually turns the eastern Pacific Ocean into a cold state. We note that the progressive rising of the thermocline from west to east reflects the recovery of the flattened thermocline, which is associated with the recovery of the equatorial trade winds. The latter are demonstrated by the eastward propagation of the equatorial easterly anomalies (*e.g.*, Wang, 1995a). This indicates that the slow eastward propagation of TDA is a manifestation of a coupled atmosphere-ocean mode (Gill and Rasmusson, 1983; Philander *et al.*, 1992). Transient Kelvin waves excited by intraseasonal wind fluctuations in the western Pacific are superposed on this low-frequency coupled mode. The possible influence of the high-frequency Kelvin waves on the low-frequency evolution was speculated by Lukas *et al.* (1984), and demonstrated by Kessler and McPhaden (1995) using a simple model, which plays a significant role in the transition of ENSO.

Similarly, the establishment of a cyclonic wind stress curl in the WNP right after the cooling (*e.g.*, 1982, 1986, and 1989) (Fig. 8a) is critical to trigger the discharge of heat content in the WNP. The anomalous westerly wind stress south of the cyclonic center deepens the thermocline in the EWP (Fig. 4, decay of the cold event), triggering the eastward migration of the heat content (deepening of the thermocline) along the equator. This eventually leads to the subsequent warming.

7. Summary

7.1 Primary results

The dominant mode of the interannual variation of thermocline depth can be approximately described by a basin-scale east-west standing oscillation. The transition from a cold to a warm phase in the seesaw oscillation features an eastward phase propagation of the thermocline depth anomalies in the equatorial waveguide. The two complementary components manifest the evolution of a coupled low-frequency basin mode. The formation of the basin mode was elucidated by the theoretical model of Cane and Moore (1981), and the numerical model by Wakata and Sarachik (1991).

Short-period and small-amplitude oscillations in the early 1990s exhibited a relatively small meridional scale in the thermocline variation. The long-period and large-amplitude cycles associated with major warmings exhibit a wider meridional scale, and involve a substantial change of heat storage in the off-equatorial regions of the western Pacific warm pool (5–15°N, 130–170°E). This region is one of the action centers in the interannual thermocline variation (Fig. 1b and Fig. 2a). The linkage between the oscillation period and the meridional scale was found as one of the characteristic features of the nonlinear oscillation in the standing oscillator model of Wang and Fang (1996), and in the coupled statistical atmosphere and Cane-Zebiak ocean

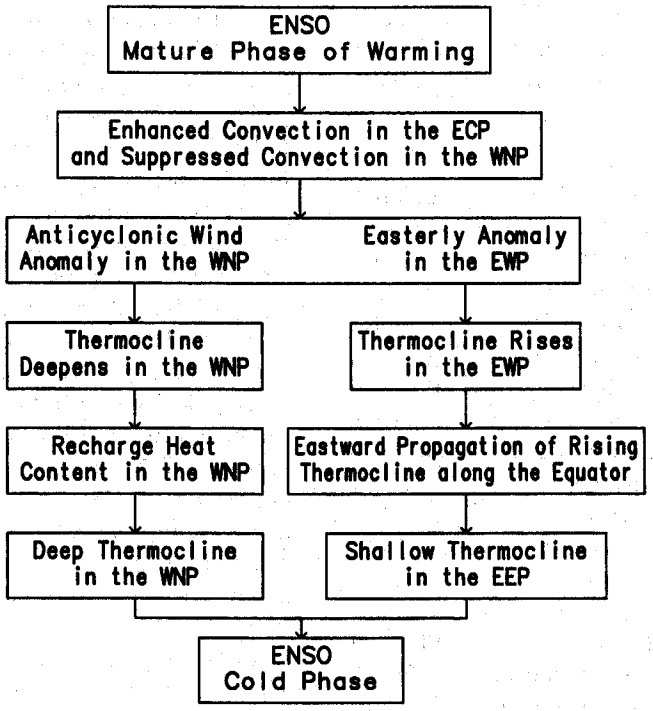

Fig. 10. Schematic diagram showing the mechanism of ENSO transition from a peak warm to a cold phase. Abbreviations WNP, EEP, and EWP stand for, respectively, the western North Pacific, the equatorial eastern Pacific, and the equatorial western Pacific.

model of Kirtman (1997). Wang and Fang (1996) showed, by scale analysis, that the meridional scale of the coupled mode reflects the magnitude of the ocean-atmosphere coupling. When the meridional scale is smaller, the lower-meridional mode equatorial Rossby waves (which propagate faster) play more active roles in adjusting the thermocline, leading to a shorter basin-wide thermocline adjustment time scale and a shorter period of oscillation. This is consistent with the idea of McCreary (1983). The dependence of the oscillation period on the meridional scale of the coupled mode suggests the critical role of the basin-wide thermocline adjustment in ENSO evolution.

The thermocline variation in the WNP plays an active role during the large amplitude long ENSO cycles. Major warm (cold) episodes appear to be preconditioned by a build up (depletion) of heat in the WNP during the preceding cold (warm) phase (Fig. 5). Both the thermocline depth tendency and the local wind stress curl show a coherent double oscillation peak with periods of 9 months and 15 months (Fig. 7). The deepening (rising) of the thermocline in that region is nearly concurrent with local anticyclonic (cyclonic) wind stress forcing (Fig. 8a). While the remotely forced Rossby wave propagation may contribute in some extent to the thermocline variation in the WNP, the local wind stress forcing appears to be a major contributor. The relative importance of the local wind stress forcing versus the remotely forced Rossby wave propagation in the thermocline variation in the WNP, as well as in other regions of the Pacific, remains a target of further investigation.

7.2 Hypothesis concerning ENSO transitions

Figure 10 summarizes the hypothesis regarding the mechanism of ENSO transition from a warm to a cold phase. During ENSO warm phases, the thermocline rises (discharging heat) in the WNP whereas it deepens in the equatorial eastern Pacific. During each major warm peak in the eastern-central Pacific, there is a rapid establishment of anticyclonic wind stress curl over the WNP. The anticyclonic wind stress curl, through Ekman motion-induced baroclinic adjustment, depresses the local thermocline and starts heat recharge in the WNP. The easterly anomalies to the south of the anticyclonic circulation extend to the equatorial western Pacific, forcing the thermocline in that region to reach the minimum depth and trigger the eastward propagation of the elevated thermocline. Concurrent with the thermocline rising in the west, there is a poleward transport of heat content in the far eastern Pacific (Fig. 9) due mainly to the propagation of the coastal Kelvin waves and associated reflected Rossby waves. This suppresses warming in the east, restoring equatorial zonal SST gradients and thus reinforcing equatorial easterlies. The enhancement of the equatorial trades supports the slow eastward propagation of the ele-

vated thermocline which eventually leads to an eastern Pacific cooling. The transition from cooling to warming follows a similar process, but with opposite anomalies.

7.3 Discussion

The proposed turnabout mechanism is independent of Rossby wave reflections at the western boundary postulated in the delayed oscillator mechanism. However, the two mechanisms may work together, rather than against each other, to determine the transition from warming to cooling or vice versa. As pointed out in Sections 4 and 5, this mechanism is relevant to relatively long period oscillation cycles and major warm events, rather than those mini-warm events with short periods. For the latter, ocean wave dynamics may play a more important role in thermocline adjustment and ENSO transition.

The key process involved in the new mechanism presented in Fig. 10 is the role of the WNP wind stress curl and associated equatorial western Pacific wind anomalies in ENSO phase transition. In a previous effort searching for precursors for the transition of ENSO, Wang (1995a) found that the anomalous sea-level pressure in the off-equatorial regions of the western Pacific reaches minimum (maximum) about 3–5 months after the peak cooling (warming). Based on analysis of sea-level pressure anomalies from 1950–1992, he showed that the 11-month running mean sea-level pressure anomalies in these regions negatively correlate with the equatorial central Pacific SST anomalies. The correlation coefficient is 0.7 at a four-month lag. The results shown in Fig. 8a are consistent with the finding of Wang (1995a) and thus are supported by a much longer observation record.

It is important to notice that the anticyclonic wind stress over the WNP is not directly associated with the equatorial central Pacific westerly anomalies during the warm peak. The anomalous westerlies and associated off-equatorial cyclonic wind stress curl is a direct response to equatorial central Pacific enhanced convective heating and can be explained by the Gill (1980) model. They generate equatorially trapped upwelling Rossby waves, probably within 5° latitudes on each side of the equator. Over the WNP, the establishment of the anticyclonic wind stress after a peak warming is indirectly teleconnected with the enhanced convection in the equatorial central Pacific. The enhanced convection in the equatorial central Pacific generates anomalous upward motion and associated anomalous Hadley and Walker circulations. The corresponding sinking branch appears to preferably occur in the WNP, because the ocean there is in an anomalously cold state. Lower SST also tends to produce higher surface pressure, favoring formation of an anticyclonic circulation (Lindzen and Nigam, 1987). The precise cause of this tropical Pacific teleconnection deserves further investigation.

The wind stress curl over the WNP is not always linked to the equatorial thermal conditions. The high-frequency nature (7–20 month broad spectral peak) of the wind stress curl is coherent with the thermocline depth tendency in the WNP (Fig. 7). The rapid restoration of the heat content is not always followed by a continuing build-up, nor is a build-up of heat from normal conditions always preceded by a rapid restoration. This induces a degree of irregularity in ENSO cycles. Situated in between the energetic monsoon system and trade wind system, the WNP surface circulation is considerably influenced by East Asian monsoon (especially the mighty winter monsoon) and midlatitude variations. That can in turn influence the build-up of heat storage in the WNP and indirectly affect ENSO evolution. The factors external to the coupled tropical ocean-atmosphere system act as stochastic forcing. This can be an important mechanism for oscillation and a source of the irregularities for ENSO as demonstrated by a coupled numerical model (Chang *et al.*, 1996) and Wang *et al.* (1998). In a coupled numerical model, if the wind stress is fully controlled by SST variations in the tropics, the thermocline variation over the off-equatorial warm pool region would not be likely to capture the observed complexity, and the simulated (predicted) ENSO cycles are likely more regular than observed.

It is worthwhile to mention that the evolution of the thermocline associated with ENSO cycles appears to have experienced an interdecadal change in the late 1970's in accordance with the change in their onset characteristics as documented by Wang (1995b). Comparison of the present results with Chao and Philander's (1993) shows that during the period prior to the 1980s (1967–1979) the thermocline variation in the Southern Hemisphere is closely associated with — whereas after 1980 it does not appear to be actively linked to — the basin-wide thermocline adjustment and the equatorial eastward propagation of thermocline depth anomalies. What causes this interdecadal variation is a subject of future investigation.

Acknowledgments

This research is supported by NOAA/GOALS and PACS programs and NSF Climate Dynamics Program (Grant No. ATM-9613776). R. Lukas acknowledges the support from NSF under grant OCE-9024452. This is the School of Ocean and Earth Science and Technology publication No. 4712.

References

Battisti, D.S. and A.C. Hirst, 1989: Interannual variability in the tropical atmosphere-ocean system: In-

fluence of the basic state and ocean geometry. *J. Atmos. Sci.*, **46**, 1687–1712.

Battisti, D.S., 1989: On the role of off-equatorial oceanic Rossby waves during ENSO. *J. Phys. Oceanogr.*, **19**, 551–559.

Bjerknes, J., 1969: Atmospheric teleconnections from the equatorial Pacific. *Mon. Wea. Rev.*, **97**, 163–172.

Boulanger, J.-P. and L.-L. Fu, 1996: Evidence of boundary reflection of Kelvin and first-mode Rossby waves from TOPEX/POSEIDON sea level data. *J. Geophys. Res.*, **101**, 16361–16371.

Cane, M.A. and D.W. Moore 1981: A note on low-frequency equatorial basin modes. *J. Phys. Oceanogr.*, **11**, 1578–1584.

Cane, M.A., M. Munnich and S.E. Zebiak, 1990: A study of self-excited oscillations in atropical ocean-atmosphere system. Part I: Linear analysis. *J. Atmos. Sci.*, **47**, 1562–1577.

Chang, P., L. Ji, H. Li and M. Flugel, 1996: Chaotic dynamics versus stochastic processes in El Niño-Southern Oscillation in coupled ocean-atmosphere model. *Physica D*, **98**, 301–320.

Chao,Y. and S.G.H. Philander, 1993: On the structure of the Southern Oscillation. *J. Climate*, **6**, 450–469.

Chelton, D.B. and M.G. Schlax, 1996: Global observations of ocean Rossby waves, *Science*, **272**, 234–238.

Firing, E., R. Lukas, J. Sadler and K. Wyrtki, 1983: Equatorial undercurrent disappears during 1982–1983 El Niño. *Science*, **222**, 1121–1123.

Gill, A.E., 1980: Some simple solutions for heat-induced tropical circulation. *Quart. J. Roy. Meteor. Soc.*, **106**, 447–462.

Gill, A.E. and E.M. Rasmusson, 1983: The 1982–1983 climate anomaly in the equatorial Pacific. *Nature*, **306**, 229–234.

Graham, N.E. and W.B. White, 1988: The El Niño cycle: A natural oscillator of the Pacific ocean-atmosphere system. *Science*, **240**, 1293–1302.

Harrison, D.E. and P.S. Schopf, 1984: Kelvin-wave-induced anomalous advection and the onset of surface warming in Niño events. *Mon. Wea. Rev.*, **112**, 923–933.

Ineson, S. and M.K. Davey, 1997: Interannual climate simulation and predictability in a coupled TOGA GCM. *Mon. Wea. Rev.*, **125**, 721–741.

Ji, M., A. Leetmaa and J. Derber, 1995: An ocean analysis system for seasonal to interannual climate studies. *Mon. Wea. Rev.*, **123**, 460–481.

Kessler, W.S., 1990: Observations of long Rossby waves in the northern tropical Pacific. *J. Geophys. Res.*, **95**, 5183–5217.

Kessler, W.S., 1991: Can reflected extra-equatorial Rossby waves drive ENSO? *J. Phys. Oceanogr.*, **21**, 444–452.

Kessler, W.S. and M.J. McPhaden, 1995: Oceanic equatorial waves and the 1991–1993 El Niño. *J. Climate*, **8**, 1757–1774.

Kirtman, B.P., 1997: Oceanic Rossby wave dynamics and the ENSO period in a coupled model. *J. Climate*, **10**, 1690–1704.

Li, B. and A.J. Clarke, 1994: An examination of some ENSO mechanisms using interannual sea level at the eastern and western equatorial boundaries and the zonally averaged equatorial wind. *J. Phys. Oceanogr.*, **24**, 681–690.

Lindzen, R.S. and S. Nigam, 1987: On the role of sea surface temperature gradients in forcing low-level winds and convergence in the tropics. *J. Atmos. Sci.*, **45**, 2440–2458.

Livezey, R.E. and W.Y. Chen, 1983: Statistical field significance and its determination by Monte Carlo technique. *Mon. Wea. Rev.*, **111**, 46–59.

Lukas, R., S.P. Hayes and K. Wyrtki, 1984: Equatorial sea level response during the 1982–1983 Niño. *J. Geophys. Res.*, **89**, 10425–10430.

Lukas, R., 1988: Interannual fluctuations of the Mindanao current inferred from sea level. *J. Geophys. Oceanogr.*, **93**, 6744–6748.

Mantua, N.J. and D.S. Battisti, 1994: Evidence for the delayed oscillator mechanism for ENSO: The "observed" oceanic Kelvin mode in the far western Pacific. *J. Phys. Oceanogr.*, **24**, 691–699.

McCreary, J.P., 1983: A model of tropical ocean-atmosphere interaction. *Mon. Wea. Rev.*, **111**, 370–387.

McPhaden, M.J., S.P. Hayes, L.J. Mangum and J.M. Toole, 1990: Variability in the western equatorial Pacific during the 1986–87 El Niño/Southern Oscillation event. *J. Phys. Ocenaogr.*, **20**, 190–208.

Meyers, G., 1982: Interannual variation in sea level near Truk Island — A bimodal seasonal cycle. *J. Phys. Oceanogr.*, **12**, 1161–1168.

North, R.G., T.L. Bell, R.F. Cahalan and F.J. Hoeng, 1982: Sampling errors in the estimation of empirical orthogonal functions. *Mon. Wea. Rev.*, **110**, 699–706.

Philander, S.G.H., R.C. Pacanowski, N.-C. Lau and M.J. Nath, 1992: Simulation of ENSO with a global atmospheric GCM coupled to a high-resolution tropical Pacific Ocean GCM. *J. Climate*, **5**, 308–329.

Qiu, B. and R. Lukas 1996: Seasonal and interannual variability of the North Equatorial Current, the Mindanao Current, and the Kuroshio along the Pacific western boundary. *J. Geophys. Res.*, **101**, 12315–12330.

Schopf, P.S. and M.J. Suarez, 1988: Vacillations in a coupled ocean-atmosphere model. *J. Atmos. Sci.*, **45**, 549–566.

Suarez, M.J. and P.S. Schopf, 1988: A delayed action oscillator for ENSO. *J. Atmos. Sci.*, **45**, 3283–3287.

Tourre, Y.M. and W.B. White 1995: ENSO signals in global upper-ocean temperature. *J. Phys. Oceanogr.*, **25**, 1317–1332.

Wakata, Y. and E.S. Sarachik, 1991: Unstable coupled atmosphere-ocean basin modes in the presence of a spatially varying basic state. *J. Atmos. Sci.*, **48**, 2060–2077.

Wallace, J.M., E.M. Rasmusson, T.P. Mitchell, V.E. Kousky and H. von Storch, 1997: On the structure of ENSO-related climate variability in the tropical Pacific: Lessons from TOGA. *J. Geophys. Res.*, **103**, 14241–14260.

Wang, B., 1992: The vertical structure and development of the ENSO anomaly mode during 1979–1989. *J. Atmos. Sci.*, **49**, 698–712.

Wang, B., 1995a: Transition from a cold to a warm state of the El Niño-Southern Oscillation cycle. *Meteorol. Atmos. Phys.*, **56**, 17–32.

Wang, B., 1995b: Interdecadal changes in El Niño onset in the last four decades. *J. Climate*, **8**, 267–285.

Wang, B. and Z. Fang, 1996: Chaotic oscillations of tropical climate: A dynamic system theory for ENSO. *J. Atmos. Sci.*, **53**, 2786–2802.

Wang, B., A. Barcilon and Z. Fang, 1998: Stochastic dynamics of ENSO. *J. Atmos. Sci.*, In press.

Wang, B., R. Wu and R. Lukas, 1998: Annual variations of the thermocline in the tropical Pacific Ocean. Submitted to *J. Climate*.

White, W.B., G. Meyers, J.R. Donguy and S.E. Pazan, 1985: Short-term climatic variability in the thermal structure of the Pacific Ocean during 1979–1982. *J. Phys. Oceanogr.*, **15**, 917–935.

White, W.B., Y. He. and S.E. Pazan, 1989: Off-equatorial westward propagating waves in the tropical Pacific during 1982–83 and 1986–87 ENSO events. *J. Phys. Oceanogr.*, **19**, 1397–1406.

Wyrtki, K., 1974: Sea level and the seasonal fluctuations of the equatorial currents in the western Pacific Ocean. *J. Phys. Oceanogr.*, **4**, 91–103.

Wyrtki, K., 1975: El Niño-The dynamic response of the equatorial Pacific to atmospheric forcing. *J. Phys. Oceanogr.*, **5**, 572–584.

Wyrtki, K., 1984: The slope of sea level along the equator during the 1982/1983 El Niño. *J. Geophys. Res.*, **89**, 10419–10424.

Yanai, M. and C. Li, 1994: Interannual variability of the Asian summer monsoon and its relationship with ENSO, Eurasian snow cover and heating. *Proc. Inter. Conf. On Monsoon Variability and Prediction.* Trieste, Italy, 9–13 May 1994. WMO/TD No. 619, Vol. I, 27–34.

Zebiak, S.E. and M.A. Cane, 1987: A model El Niño-Southern Oscillation. *Mon. Wea. Rev.*, **115**, 2262–2278.

Zhang, R.-H. and S. Levitus, 1997: Interannual variability of the coupled tropical Pacific ocean-atmosphere system associated with the El Niño/Southern Oscillation. *J. Climate*, **10**, 1312–1330.

水温躍層調節とENSO位相変化における北西太平洋風変動の役割

B. Wang・R. Wu・R. Lukas

(School of Ocean and Earth Science and Technology, University of Hawaii at Manoa)

17年間分 (1980–1996) の熱帯太平洋水温躍層の解析は、1990年代初期の変動が短周期 (約18カ月) で南北スケールも比較的に小さいのに対し、1980年代ではENSOの大規模な変動と関連し周期は長く (4–5年) 南北スケールはより大きいことを示している。水温躍層深度の経年変動の卓越モードは、近似的には遷移期に赤道ウェーブガイドに生じる水温躍層深度東方伝播を伴う東西のシーソー振動で表現される。

大規模で長周期のENSOは、北西太平洋 (NWP) (5–15°N, 130–170°E) の貯熱量の実質的な変化を伴う。水温躍層変位とNWPにおける風カールの変化傾向は8–20カ月の幅広いスペクトルピークをもちコヒーレントである。水温躍層の下降 (上昇) は局所的な高気圧性 (低気圧性) 風応力と同位相であり、この事実は水温躍層調節においてその場での風強制が本質的である事を示唆している。

西太平洋の海上風の変動がENSOサイクルの位相変化に重要な役割をはたしていることを提唱する。暖かい時期の完熟期に、WNPの高気圧性風応力カールが急速にできあがる。それがWNPの水温躍層を深めることにより、ウォームプールでは熱を再び溜め始める。その間に高気圧の南側の東風アノマリーが赤道太平洋西部の水温躍層を押し上げて、赤道に沿う浅い水温躍層の東方伝播の引き金となり、その結果東部の低温下を導く。冷たい時期に於ける完熟期での降温から昇温への転移は、同様の過程によるが偏差の符号は逆である。